Journal of Alloys and Compounds 509 (2011) 2355–2359

Contents lists available at ScienceDirect

Journal of Alloys and Compounds

journal homepage: www.elsevier.com/locate/jallcom

Compressive yield strength of the nanocrystalline Cu with Al_2O_3 dispersoid

Seung J. Hwang*

Department of Materials Science and Engineering, Daejin University, Pocheon, Kyung-gi 487-711, Republic of Korea

ARTICLE INFO

Article history:
Received 20 September 2010
Received in revised form 1 November 2010
Accepted 3 November 2010
Available online 10 November 2010

Keywords:
Nanostructured materials
Mechanochemical processing
TEM metallography
Mechanical properties

ABSTRACT

Nanocrystalline (nc) Cu with Al_2O_3 dispersoid (~4 vol.%) was successfully synthesized by simple cryo-milling at 210 K with a mixture of Cu_2O, Al, and Cu elemental powders. The milled powder was consolidated by hot pressing (HP) at 1123 K and 50 MPa for 2 h. TEM (Transmission Electron Microscopy) work revealed that both of the milled powder and the hot pressed (HPed) materials were comprised with a mixture of the nc-Cu and homogeneous distribution of Al_2O_3 dispersoids. The compressive and micro Vickers hardness tests were performed on the HPed materials (nanocrystalline Cu with 4 vol.% of Al_2O_3 dispersoid) at room temperature to characterize the mechanical properties of the materials. The compressive yield strength of the materials was as high as 863 MPa; the micro Vickers hardness 2600 MPa. The results of the mechanical tests apparently show that the relationship between the yield strength and the micro hardness of the HPed materials is in well agreement with Tabor's rule, $H_v = 3\sigma_y$ in MPa. The grain size of the nc-Cu was estimated by XRD using Scherrer's formula and TEM observation; the Al_2O_3 dispersoid size was measured from element mapping by STEM–EDS (Scanning Transmission Electron Microscopy–Energy Dispersive Spectroscopy) works. An attempt was made to quantify the possible strengthening effects of the nc-Cu materials with Al_2O_3 dispersoid. Two strengthening mechanisms were proposed for high hardness and yield strength of the materials, i.e., grain size and dispersion hardening effects.

1. Introduction

It is widely known that the mechanical behavior of the nc-materials is characterized by a significant increase in yield strength and decrease in ductility [1–5]. With nc-materials of a various range of the grain size, the tensile/compressive test results indicated that the Hall–Petch mechanism is obeyed down to 20 nm below which the rule is no longer dominant [6–10]. A great deal of attentions has been paid on the so-called "break down" of the Hall–Petch relationship at the critical grain size [6–11]. By decreasing the grain size to the on-set of the break-down, the deformation mechanism of the nc-materials may switch from the dislocation glide to grain boundary slip [7,11]. It is also proposed that a materials with grain size less than ~20 nm leads to the beginning of the grain boundary sliding from the dislocation activity while deformed [12,13].

In this study, a type of the nc-Cu materials with the Al_2O_3 was produced by the reactive milling at 210 K to attain the minimum size of the Cu grain and Al_2O_3 dispersoids, followed by the HP to consolidate the milled powder. Two strengthening mechanisms are considered for the high yield strength of the materials: grain refinement and dispersion hardening. The purpose of this work is to estimate the contributions of the individual strengthening mechanism to the total yield strength in the nc-Cu materials with the Al_2O_3 dispersoid, assuming that the Hall–Petch relationship and Orowan effect are valid down to the grain size of 20 nm.

2. Experimental

A mixture (100 g) of elemental powders, Cu (Aldrich, −200 mesh, 99%), Cu_2O (Sigma–Aldrich, −325, 97%) and Al (Johnson Matthey, −40 + 325 mesh, 99.8%), was prepared for reactive-milling at a high energy attritor mill for 8 h in the high purity argon atmosphere with ball to powder ratio 15:1 at 210 K using liquid nitrogen. To obtain the desired composition (~4 vol.% Al_2O_3) of the materials, the elemental powders were measured in a molar proportion according to the reaction as follows:

$$3Cu_2O + 2Al + 77.3Cu \rightarrow 83.3Cu + Al_2O_3 \quad (1)$$

Milling process was periodically monitored by XRD to completion of the reaction. The result of XRD patterns of milled powder obtained from milling times of up to 8 h is shown in Fig. 1.

The contamination of impurities is always a concern in the milling processes. It was presupposed that most of oxygen was tied up with Al, resulting in the formation of Al_2O_3 and rest of gas elements is evacuated during the HP. Moreover, in order to minimize the contamination from the grinding ball and chamber wall, the pre-milling with pure Cu powder was performed to flush out the possible contamination before the main milling. The contaminations of the materials were examined by the XRD and EDS for the milled powder and the HPed materials. There was any evidence of peak shift or significant impurity pick-ups nowhere; it is supposed that the level of Fe contamination is very low and undetectable due to the limited solubility between the Fe and Cu element if involved any.

A button type of sample (16 mm, Φ × 12 mm) was prepared by vacuum hot press (HP) at the 1123 K and 50 MPa in argon atmosphere for 2 h from the milled powder.

* Tel.: +82 31 539 1984.
E-mail address: sjhwang@daejin.ac.kr

0925-8388/$ – see front matter © 2010 Elsevier B.V. All rights reserved.
doi:10.1016/j.jallcom.2010.11.017

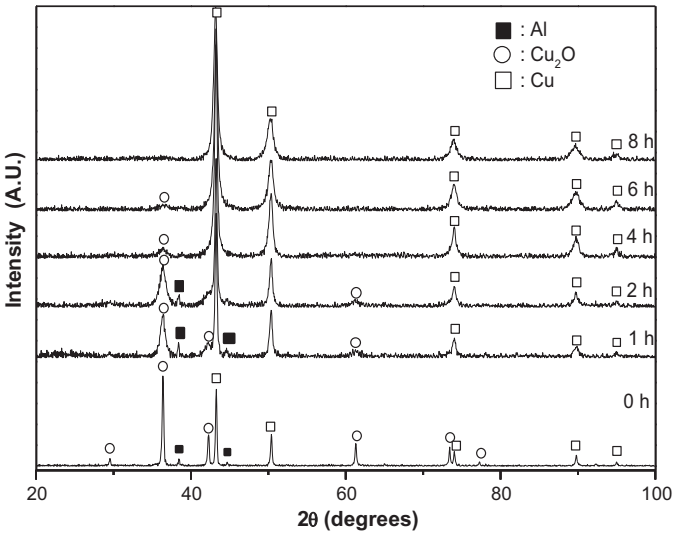

Fig. 1. XRD patterns of the milled powder obtained from milling times of up to 8 h indicating the milling completed with a mixture of Cu and Al_2O_3.

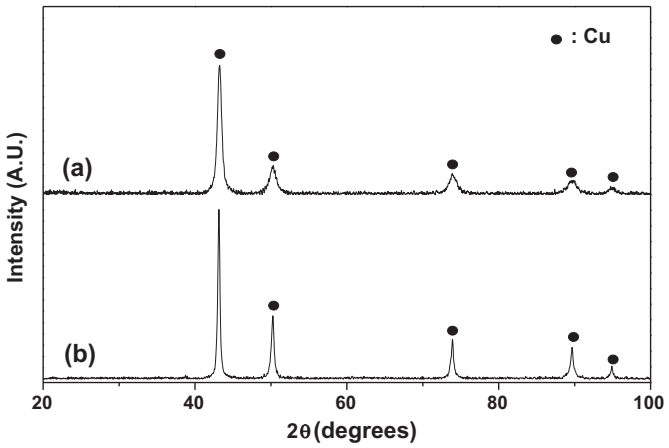

Fig. 2. XRD patterns of the milled (a) and the HPed (b) nc-Cu with Al_2O_3 dispersoids (the peaks of Cu are clearly identified while those of Al_2O_3 are insignificant).

The vol.% of the Al_2O_3 in the HPed materials was estimated by calculation, assuming that all Al and O react to form Al_2O_3 during the reactive milling; a quantitative image analysis of STEM micrographs was also done to measure the volume fraction, dispersoid radius and mean planar separation of Al_2O_3 in the materials. The grain size of nc-Cu was calculated by the full width at half maximum (FWHM) of Cu (1 1 1) diffraction peak using Scherrer's formula [16]. The mean intercept method was also performed to determine the Cu grain size on a TEM picture. The microstructure and phase identification of the milled powders and the HPed materials were conducted by TEM and XRD, using Cu Kα radiation.

The micro Vickers hardness test and compressive test were performed on the HPed materials. The compressive tests were done in a floor model Instron with a 5 tonnes load cell at room temperature. The specimens were machined by Electro Discharge Machine (EDM) and ground with low stress grinder in order to achieve smooth, flat and parallel cylinders with 11 mm long by 5 mm diameter. The specimens were then deformed between hardened tool steel plates using Teflon tapes to reduce barreling. Load-elongation data were converted to true stress and true strain by digitizing chart recording with assumption of conservation of volume. The nominal strain rate for the tests was typically 1×10^{-3}/s. The arithmetic averages (MPa) of 0.2% off-set yield strengths and H_v values of the materials exclusive of the highest and the lowest from 10 measurements were reported along with the standard deviation. The details of the processing and characterizing techniques are described in elsewhere [14–16].

3. Results and discussion

Fig. 1 shows XRD patterns of the milled powder obtained from milling times of up to 8 h. The result illustrates that Cu_2O and Al peaks progressively disappeared with increasing milling time; the counts of these peaks were well below the resolution limit of XRD after 6 h milling, which is indicative evidence of the milling completed. Fig. 2 illustrates the XRD patterns of the milled powder and the HPed materials. In both of the XRD pattern, the peaks of Cu are clearly identified while those of Al_2O_3 are insignificant. This is likely due to the difference in absorption coefficient of the Cu and Al element on the XRD patterns as explained by Leonard and Koch for the milled powder [17]. However, with the result of STEM–EDS mapping, the presence of Al_2O_3 dispersoids was obviously evidenced; the size and vol.% of the dispersoid are well in agreement with the calculation as reported previously [14,15]. In Fig. 3, the TEM microstructures of the milled powder are illustrated; the Al_2O_3 dispersoids and twins by the reactive milling are presented. It is noticed that the nano Cu powders (a) were agglomerated and dispersoids were embedded in Cu particle (b).

Table 1
The actual yield stress of the nc-Cu with Al_2O_3 dispersoid obtained from the compressive tests and the calculated yield stress from the micro hardness data.

Micro hardness (MPa),	Yield stress (calculated, $H_v/3$, MPa),	Yield stress (tested, MPa)
2600 ± 79	860 ± 26	863 ± 38

The micro Vickers hardness test was performed on the milled powder and the HPed materials. As shown in Table 1, the hardness of the HPed materials was a little higher than that of the milled

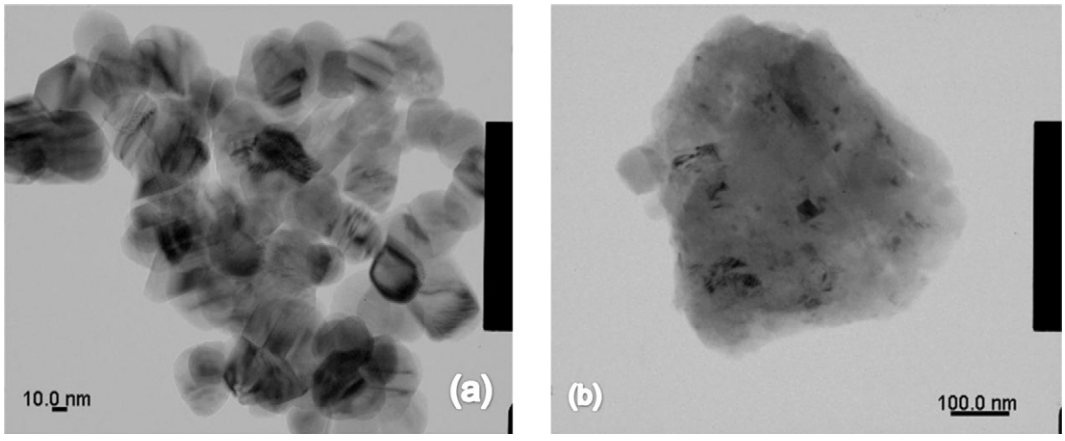

Fig. 3. TEM micrographs of the milled powder for 8 h showing the Al_2O_3 dispersoid and twins produced by reactive milling (lower magnification (a) and higher magnification (b)).

Table 2
Grain size of Cu, vol.% of Al_2O_3, dispersoid size of Al_2O_3 and mean planar separation of the dispersoids for the quantitative analysis.

Grain size of Cu (d) (Scherrer's/intercept method, nm)	Volume fraction of Al_2O_3 (f) (calculated/measured, %)	Dispersoid radius (r) (measured, nm)	Mean planar separation (λ) (calculated/measured, nm)
$25.1 \pm 0.3/21.5 \pm 4.2$	4.1/4	4	$29/24 \pm 6$

power (2530 ± 71 MPa). The grain size of the HPed materials was estimated by measuring FWHM of Cu (1 1 1) diffraction peak using Scherrer's formula [18]. The result of the measurement is given in Table 2. It is worth noting that the sizes of the Cu grain have not coarsened (from 12.7 nm to 21.5 nm) very much even at high temperature (1123 K) during HP processes. It is most likely due to the presence of the dispersoids, which leads to the retention of the nc-grains of Cu by pinning grain boundaries.

Fig. 4 illustrates the TEM bright field image and the corresponding electron diffraction pattern obtained from the HPed materials. An attempt was made to identify the phases in the HPed materials by indexing electron diffraction pattern taken in the representative area. The diffraction analysis reveals that most of the diffracted beams (rings) are attributed to the mixture of nano-sized Cu and Al_2O_3 dispersoids. Separation of Al_2O_3 phase from the Cu phase was performed on the dark field image of the HPed materials by taking only electron diffraction beams of Al_2O_3 (1 0 4) and (1 1 0) where the dispersoids were observed. The dark field image (Fig. 5b) of the materials shows the homogeneous distribution of the dispersoids with the uniform size. A STEM image (Fig. 6a) of the HPed materials confirmed that a nano size distribution of the Al_2O_3, with some coarse particles. In previous work [14,15], the element mapping images of Al and Cu also clearly showed the uniform size distribution of Al_2O_3 in nano size. This is well in agreement with the result of HRTEM where the dark phases are most likely the Al_2O_3 dispersoids (Fig. 6b). The grain size measurement of Cu with bright field images was performed on the HPed materials (Fig. 4) by mean intercept method. The average grain size estimated from the method is of 21.5 nm, while a few grains approaching to a micrometer in diameter were rarely present; results of grain size measurement are given in Table 2.

A typical compressive true stress–strain curve of the HPed materials at room temperature is presented in Fig. 7. The value of 0.2% off-set yield stress for the each test was taken from the stress–strain curve. Hence, the arithmetic average of yield stress from the results of 8 compressive tests was reported with the standard deviation in Table 1.

The results presented indicate that the HPed nc-Cu with Al_2O_3 dispersoid showed a yield strength and micro hardness as high as 863 MPa and 2600 MPa in the average, respectively. In comparison with micro grained Cu (σ_y, 56 MPa [5]), this is remarkable increment of the mechanical properties of the nc-C. It is noteworthy that relationship between the yield strength and hardness is well in agreement with the Tabor's rule, $H_v = 3\sigma_y$. It seems to be under-

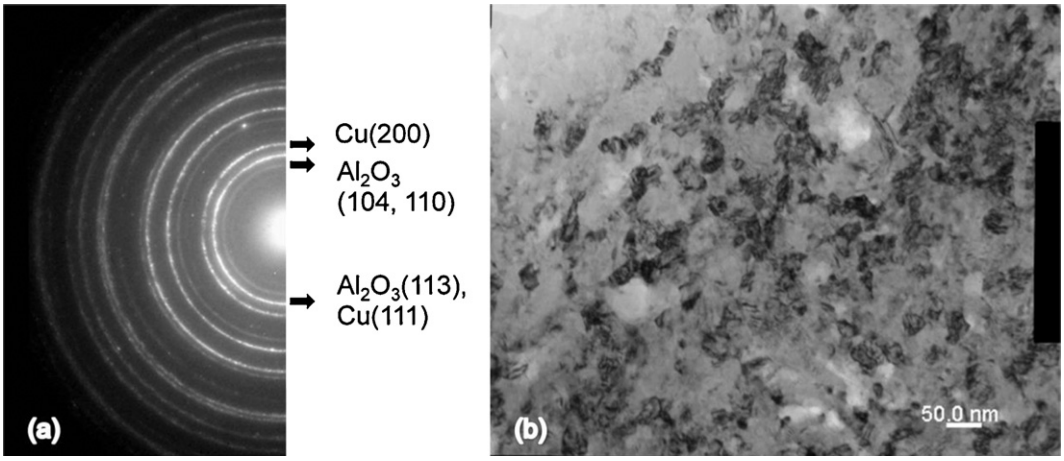

Fig. 4. Bright field image of TEM (b) and corresponding SADP (a) with indexes illustrating the presence of nc-Cu and Al_2O_3 dispersoids.

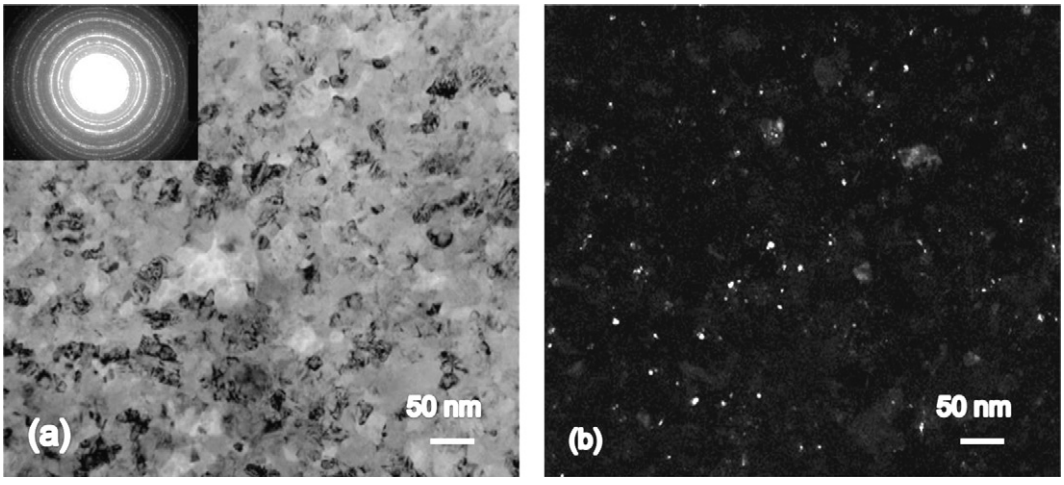

Fig. 5. TEM bright field image (a) and dark field image (b) by taking only electron diffraction beams of Al_2O_3 (1 0 4) and (1 1 0) in the SADP (inset of the left picture).

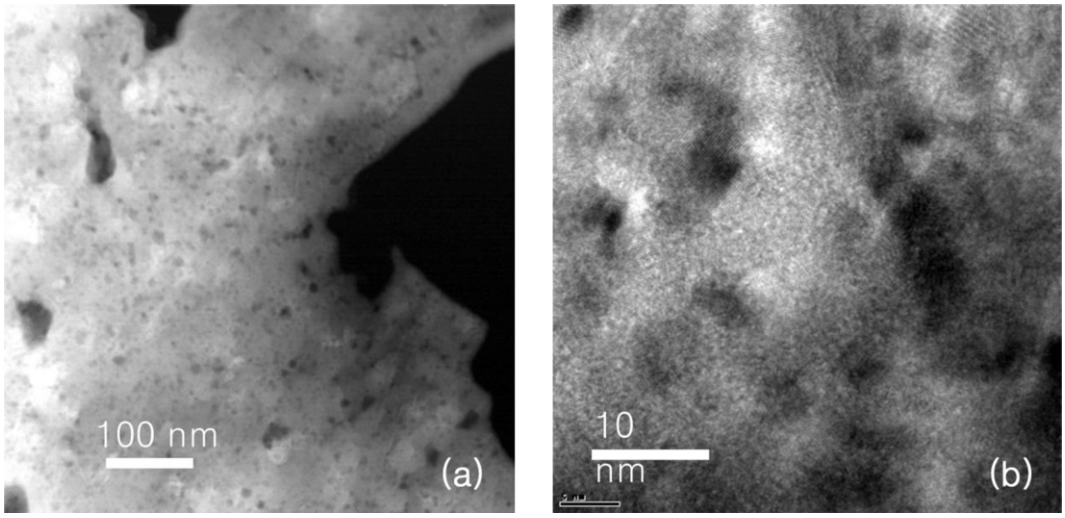

Fig. 6. Micrograph of STEM (a) and HRTEM (b) showing the size distribution of nano sized Al_2O_3 dispersoids in the nc-Cu matrix [15].

standable that the high mechanical properties of the materials are due to the grain size and dispersion effects.

Now, we are able to discuss the strengthening mechanisms which may impact on the yield strength of the nc-materials in this study. There are two possible strengthening mechanisms to be considered in the nc-Cu with dispersoid, assuming that the Hall–Petch relationship and Orowan effect are still effective down to the grain size of the materials investigated. These are:

1 Dispersion hardening;
2 Grain size strengthening.

These strengthening mechanisms are additive and total yield strength of the nc-Cu should be considered the sum of these mechanisms. Firstly, the contribution of the Al_2O_3 dispersoids present in the nc-Cu to the overall strength of the materials should be considered. The high yield strength of dispersion hardened alloys is usually explained by the Orowan mechanism for the interaction of dislocations with insoluble dispersoids. The mean distance between the dispersoids was estimated by calculation of Eq. (2) as

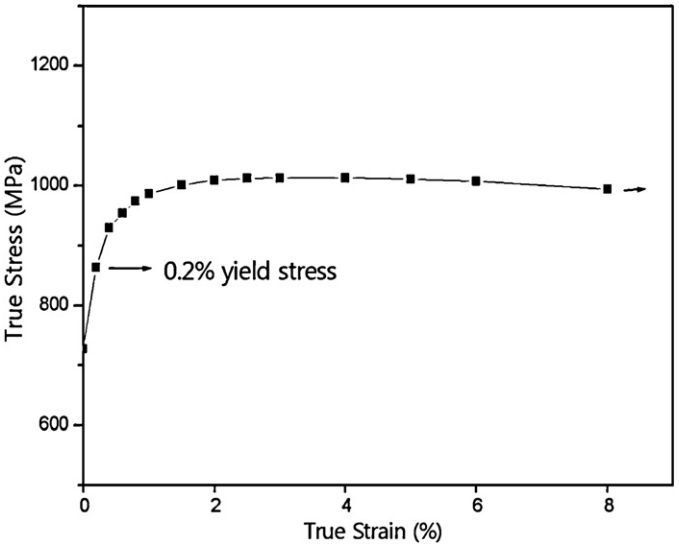

Fig. 7. A typical compressive true stress–strain curve of the HPed nc-Cu with Al_2O_3 dispersoid at room temperature exhibiting a yield strength as high as 863 MPa with a significant compressive ductility (>8%).

well as by direct measurement on the TEM micrographs. The estimated values of the separations by the both of techniques were well in agreement (see Table 2). It would be reasonable to use the mean distance between the dispersoids determined by calculation for analysis in that the actual separation (in 3 dimension) of the dispersoids is always larger than it appears on the TEM micrograph (2 dimension). Given the volume fraction (f) and dispersoid radius (r), the mean distance between the dispersoids (λ) of Al_2O_3 dispersoid can be calculated as shown in Eq. (2). If an Orowan type mechanism is assumed, the increment in yield strength of the materials, $\Delta\sigma_d$, due to the non deformable dispersoids with the mean distance between the dispersoids (λ), is as followed [19,20]:

$$\Delta\sigma_d(\text{MPa}) = 0.84\left(\frac{2T}{b\lambda}\right), \quad \text{where } \lambda = r\left(\frac{2\pi}{3f}\right)^{1/2} \tag{2}$$

With the size and volume fraction of the dispersoids in Table 2, the Orowan strengthening effect of the nc-Cu with Al_2O_3 dispersoid, $\Delta\sigma_d$, is found to be 226 MPa using $T = 1.0 \times 10^{-9}$ N, and $b = 2.56 \times 10^{-10}$ m (T, b: line tension and burgers vector of the dislocation, respectively) [20]. This is only 22% of the overall yield stress; the contribution of the dispersion effect is a minor in the yield strength of the materials. In this study, it is proposed that the nano sized (~4 nm) dispersoids do not play a major role to increase the yield strength of the materials but to retain the grain size by the pinning effect of grain boundaries, which leads to indirect strengthening effect as a results.

Secondly, let us consider the grain refinement strengthening mechanism contributing to the strength of the materials. The grain size of the HPed materials was measured using the Scherrer's formula with the FWHM of Cu (1 1 1) diffraction peak. For the confirmation of the Cu grain size, the mean intercept method was done to measure the grain size of the materials for the same materials. The results of the measurement are presented in Table 2 with a reasonable agreement. The influence of Cu lattice strain on broadening of the diffraction lines was not taken into account because it is most likely that the strain effects would be eliminated by annealing at HP process. Using the data from the mean intercept method, we found that the Hall–Petch equation given in Eq. (3) estimated the increment of the yield stress of the HPed materials due to the grain size as follow:

$$\Delta\sigma_g(\text{MPa}) = 25.5 + 3478.5(d)^{-1/2}\ \text{nm}^{1/2} \tag{3}$$

It is calculated that the yield strength increment due to the grain size of the materials in this study is 775 MPa using the mean inter-

cept method (21.5 nm, Table 2). The estimated value of the yield strength by Eq. (3) is reasonably in agreement with other experimental works, i.e., ~688 MPa for $d = \sim 54$ nm [1], 760 MPa for $d = \sim 30$ [3], and 850 MPa for $d = \sim 20$ nm [4] where they report yield strength with a various grain size of Cu.

The overall strength (σ_o) of the HPed nc-Cu with Al_2O_3 dispersoids is the sum of grain size and dispersion strengthening effects:

$$\sigma_o = (\Delta\sigma_g) + (\Delta\sigma_d)775 + 226 = 1001\ \text{MPa} \quad (4)$$

However, the validity of the dispersion hardening effect in the nc-Cu with Al_2O_3 system is raised in that there is still no conclusive evidence of the reaction between dislocations and dispersoids such as Orowan loop or the departure side of pinning in the nc-materials in this study. It is not understood yet how the mobile dislocations react with the dispersoids, most of which are preferentially found not in the grains but at the grain boundaries for their great quantity in nc-materials. Perhaps, the Orowan effect is invalid in this case for the reason above, giving rise to insignificant contribution to the strengthening. To fully support the explanation of the yield strength increase by the dispersion hardening effect in this study, additional works are required for deep understanding of the strengthening and deformation mechanisms of the nc-materials with the various sizes of grains and dispersoids.

4. Conclusion

In summary, it is concluded that the compressive 0.2% yield stress of the HPed nc-Cu with the 4 vol.% of the Al_2O_3 dispersoids is as high as 863 MPa; the micro hardness 2600 MPa, which obey well Tabor's relation ($H_v = 3\sigma_y$ in MPa) at room temperature. The result of this study shows that the incremental yield strength of the materials predicted by Hall–Petch equation is practically in agreement with the results of the experimental works where they report the yield strength of nc-Cu with a similar grain size. The estimation of the contribution of the strengthening mechanisms suggests that the grain size effect give rise to a major contribution to total yield strength of the nc-Cu with Al_2O_3 dispersoid (775 MPa) while a minor is attributed to the dispersion hardening effect (226 MPa) due to the Al_2O_3 dispersoid only if the validity of the Orowan effect assumed.

Acknowledgement

This work was supported by the Daejin University Special Research Grants in 2009.

References

[1] S. Cheung, E. Ma, Y.M. Wang, L.J. Kecskes, K.M. Youssef, C.C. Koch, U.P. Trociewitz, K. Han, Acta Mater. 53 (2005) 1521–1533.
[2] C.C. Koch, Scr. Metall. Mater. 49 (2003) 657–662.
[3] Y.M. Wang, K. Wang, D. Pan, K. Lu, K.J. Hemker, E. Ma, Scr. Mater. 48 (2003) 1581–1586.
[4] P.G. Sanders, C.J. Youngdahl, J.R. Weertman, Mater. Sci. Eng. A234–236 (1997) 77–82.
[5] K.M. Youssef, R.O. Scattergood, K.L. Murty, C.C. Koch, Appl. Phys. Lett. 85 (2004) 929–931.
[6] T.G. Nieh, J. Wadworth, Scr. Metall. Mater. 25 (1991) 955–958.
[7] J. Schiotz, K.W. Jacobsen, Science 301 (2003) 1357.
[8] C.A. Schuh, T.G. Nieh, H. Iwasaki, Acta Mater. 51 (2003) 431–443.
[9] A.J. Detor, C.A. Schur, Acta Mater. 55 (2007) 371–379.
[10] J.R. Weertman, Mater. Sci. Eng. 166 (1993) 161–167.
[11] Y.J. Wei, C. Su, L. Anland, Acta Mater. 54 (2006) 3177–3190.
[12] J.R. Trelewicz, C.A. Schuh, Acta Mater. 55 (2007) 5948–5958.
[13] Y.T. Zhu, T.G. Landon, Mater. Sci. Eng. 409 (2005) 234–242.
[14] J.-h. Lee, S.J. Hwang, Rev. Adv. Mater. Sci. 18 (2008) 289–292.
[15] S.-I. Hahn, S.J. Hwang, J. Alloys Compd. 483 (2009) 207–208.
[16] S.J. Hwang, J.-h. Lee, Mater. Sci. Eng. A405 (2005) 140–146.
[17] R.T. Leonard, C.C. Koch, Scr. Mater. 36 (1997) 41–46.
[18] B.D. Cullity, S.R. Stock, Elements of X-ray Diffraction, 3rd ed., Prentice Hall, Upper Saddle River, NJ, 2001.
[19] J.W. Martin, Micromechanisms in Particle Hardened Alloys, Cambridge University Press, Cambridge, UK, 1980, pp. 60–98.
[20] B. Tian, P. Liu, K. Song, Y. Li, Y. Liu, F. Ren, J. Su, Mater. Sci. Eng. A435–436 (2006) 705–710.